

Density Control by Second Harmonic X Mode ECRH in LHD

Shin KUBO¹⁾, Takashi SHIMOZUMA¹⁾, Kenji TANAKA¹⁾, Teruo SAITO¹⁾,
Yoshinori TATEMATSU¹⁾, Yasuo YOSHIMURA¹⁾, Hiroe IGAMI¹⁾, Takashi NOTAKE¹⁾,
Shigeru INAGAKI³⁾, Naoki TAMURA¹⁾ and LHD Experimental Group¹⁾

¹⁾National Institute for Fusion Science, Toki 509-5292, Japan

²⁾Research Center for Development of FIR Region, Fukui Univ.,

³⁾Research Institute of Applied Mechanics, Kyushu Univ., Kasuga 816, Japan

(Received 26 October 2007)

Density clamping or pump out phenomena are observed both in tokamaks and helical systems during high power heating, in particular electron cyclotron resonance heating. If the change of the particle flux and resultant electric field can be localized by the local heating of ECRH, it can be a powerful nob for the control of the particle as well as the heat transport. High power density local second harmonic X (X2) mode ECRH is applied to NBI target plasma at ripple top and bottom resonance conditions so as to keep the identical power deposition profile for both cases to distinguish the ECRH induced flux and enhanced diffusion due to the electron temperature rise. Experimental results indicates that the ECRH induced flux can explain the difference of the density clamping between ripple and bottom heating.

Keywords: ECRH, density pump out, density control, direct loss, radial electric field

1 Introduction

Density clamping or pump out is the common phenomena in tokamaks and helical systems during high power density heating, in particular electron cyclotron resonance heating. These phenomena are discussed in terms of the enhanced electron diffusion induced by the perpendicular acceleration in velocity space and the resultant electric field [1] [2] [3]. It is also pointed out that the change in the electron temperature profile can enhance radial flux due to a non zero off-diagonal term in the transport matrix which can be appreciable by the excitation of turbulent instabilities like trapped electron modes[4]. If the change of the particle flux and the resultant electric field can be localized by the local heating of ECRH, it can be a powerful nob for the control of the particle as well as the heat transport. In order to distinguish the effect of enhanced electron flux directly driven by the ECRH or enhanced diffusion due to the change in the electron temperature or off-diagonal transport matrix, series of experiments are performed. High power density local second harmonic X (X2) mode ECRH is applied to NBI target plasma at ripple top or bottom resonance for the different ripple conditions. The difference in the transient behavior of density profile is observed between top and bottom heating, or high and low ripple configurations. X2 mode is selected because the perpendicular acceleration is more enhanced in X2 than in fundamental O mode (O1) mode. The role and the mechanism of ECRH induced particle flux in the particle and heat transport is discussed based on these phenomena. Such degradation of particle confinement is also observed in a tan-

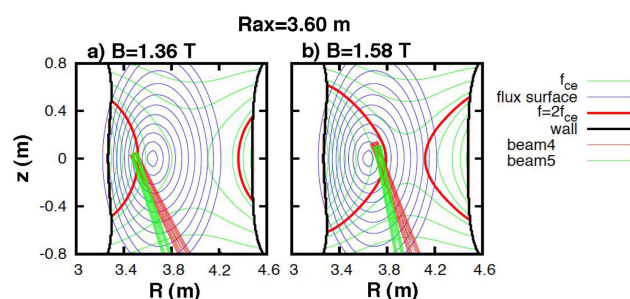


Fig. 1 Vertically elongated cross section of Mod-B, flux surfaces, second harmonic resonance layers and ECRH beams for ripple a) top and b) bottom heating geometries. for $R_{ax} = 3.60m$.

gential negative ion neutral beam (N-NB) heated plasma in LHD for low density discharges, where the electron heating is dominant but heating in parallel to the magnetic field. Such observations also support the enhancement of the off-diagonal transport term. In order to distinguish both effects, series of experiments are performed. High power density second harmonic local ECRH is applied on the ripple top or bottom resonance position where the width of the loss cone is wider for bottom than that for top, but expected power deposition profile is identical to each other in LHD.

2 Experimental results

2.1 Ripple top and bottom heating condition

In order to enhance the difference in the electron flux by ECRH, the heating positions and magnetic field strength

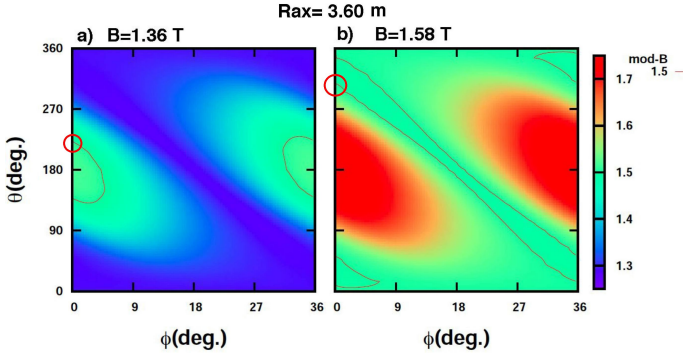


Fig. 2 Mod-B contour on toroidal poloidal plane on $\rho = 0.3$ of $R_{ax} = 3.60m$ configuration for ripple a) top and b) bottom heating geometries. Thin blue lines indicate the second harmonic resonance position for 84 GHz, and red circle indicates deposition region.

are selected so that the toroidal ripple top and bottom are heated but keeping the identical normalized radial position on the same vertically elongated cross section. The magnetic field strength and ECRH injection angles are adjusted to meet the second harmonic resonance condition (1.5 T for 84 GHz) at desired position as shown in Figs. 1 and 2. Figure 1 are shown the vertically elongated cross section of LHD with the Gaussian beams from bottom for the magnetic field strength of a) 1.36 T and b) 1.58 T for the $R_{ax} = 3.60 m$ configuration. The second harmonic resonance layer is also shown in thick red lines. Strong interactions are expected at the cross section between the injected beam and the resonance. The power deposition profiles estimated from the multi-raytracing code are confirmed to be identical and sharp at normalized minor radius, $\rho=0.3$, for both cases. Relative power deposition region on the expanded $\rho=0.3$ flux surface are shown by red circles in Fig. 2 for both magnetic field cases. Here, the strength of the total magnetic field (Mod-B) is expressed in color scale on the plane of toroidal and poloidal angle at $\rho=0.3$ flux surface for a) ripple top and b) bottom heating condition. Typical time evolutions of the plasma discharge are shown in Fig. 3. Ripple top and bottom second harmonic heating under the condition shown in Figs. 1 and 2 superposed on the base NBI plasma. A set of discharge is selected for the initial density is almost the same. Time response of the averaged density clearly differs in the case of ripple bottom heating case from that of bottom case. For both cases, the temperature responds rapidly within the time of 0.05 sec.

In order to confirm the ECRH clamping effect due to the ripple and bottom heating, similar experiments are performed for the smaller ripple condition. Here, the configuration $R_{ax} = 3.75 m$ is chosen as a reference. In Figs. 4 and 5 are shown the injection condition and Mod B structure in relation to the heating region. As is seen from Fig. 2 and 5, the ripple ratio is 0.15 and 0.1 for the case of $R_{ax} = 3.60$ and 3.75 m, respectively. Typical discharge waveforms are shown in Fig. 6 for ripple top and bottom cases. The

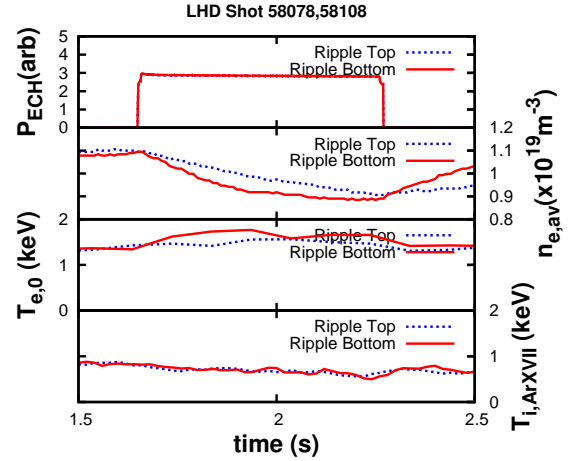


Fig. 3 Temporal evolutions of line averaged density, central electron and ion temperature for ripple top (dotted lines) and bottom (thick lines) ECRH on NB heated discharge.

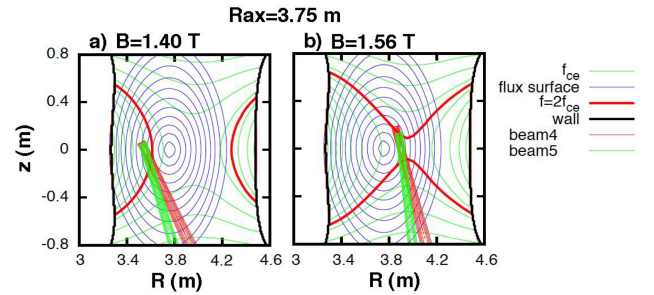


Fig. 4 Vertically elongated cross section of Mod-B, flux surfaces, second harmonic resonance layers and ECRH beams for ripple a) top and b) bottom heating geometries, for $R_{ax} = 3.75m$.

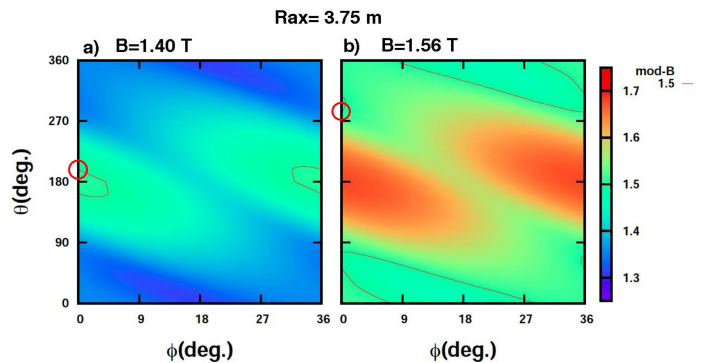


Fig. 5 Mod-B contour on toroidal poloidal plane on $\rho = 0.3$ of $R_{ax}=3.75 m$ configuration for ripple a) top and b) bottom heating geometries. Red line indicates the resonance position.

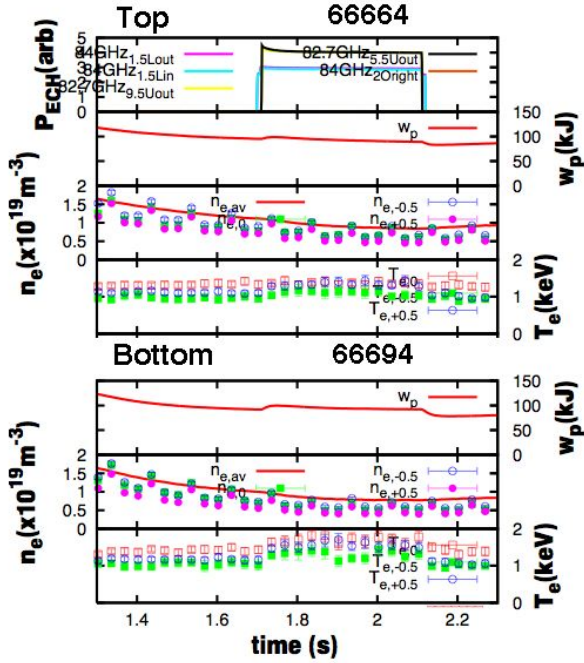


Fig. 6 Temporal evolutions of line averaged density, central electron and ion temperature for a) ripple top and b) bottom ECRH on NB heated discharge.

increases in the electron temperature and stored energy in both cases are clear, but the clamping effect is weak for both cases. The difference of clamping effect for both cases needs to be analyzed more in detail, but it is clear from the comparison with $R_{ax}=3.60$ m configuration that the density clamping is strongly related to the magnetic ripple rate at the heating region, implying that the ECRH related physics plays an important role in the clamping phenomena.

2.2 Detailed comparison of electron temperature and density profile for $R_{ax} = 3.60$ m configuration

In Fig. 3 are shown the time evolutions of the density, central electron and ion temperature in response to the ECRH on NB heated plasma for ripple top and bottom resonance heating conditions. In both cases, density decrease is observed by applying ECRH, but the time behavior of the decrease in the density clearly changes as the heating position. The line averaged density decreases faster in ripple bottom heating case than in top one. The decrease rate saturates in the time constant of 200 ms for the bottom heating case, while that for the top heating case keeps constant during the ECRH injection of 500 ms. Electron temperature increases within 100 ms and keeps almost constant during the injection for both cases. The profile changes of density reconstructed from a multi-chord FIR interferometer are shown in Fig.7. It should be noted that the density drops at $\rho > 0.4$ but central part does not affected by the ECRH injection for top heating case, while that drops al-

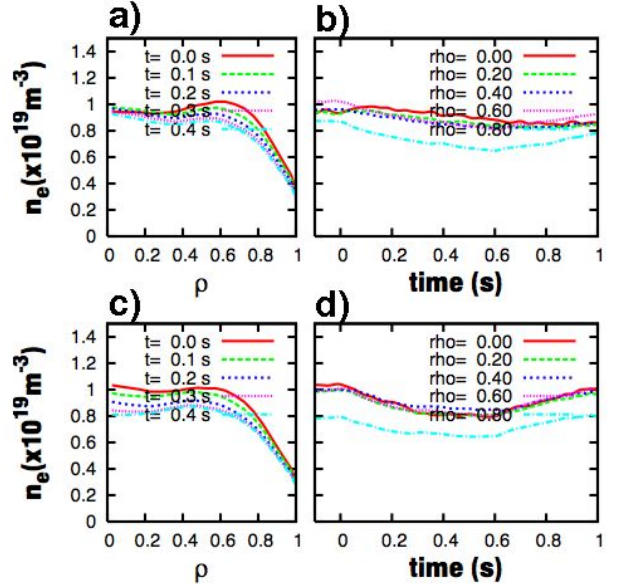


Fig. 7 Density profile at several time slices after ECH injection [a) and c)]. Time evolutions of the density at several spatial points b), and d) for ripple top [a) and b)] and bottom [c) and d)] heating cases.

most whole region for bottom heating case. The change of the electron temperature profile at several timing during the ECRH phase and the temporal evolutions at several radial positions are shown in Fig. 8. The temperature increase of the central region for the case of ripple bottom due to the ECRH is larger as compared with the ripple top case. In both cases, the profile change occurs in less than 100 ms and kept almost constant after 100 ms from the ECRH injection. This means that the change in the density profile evolutions after 100 ms of ECRH injection are attributed to the diagonal term and direct flux due to the ECRH in the electron diffusion.

3 Discussion

Neglecting the source and sink term other than that due to ECRH, diffusion equation can be written by electron density $n_e(r, t)$ and temperature profiles $T_e(r, t)$ as

$$\Gamma_e(r, t) = D_{e,n}(r, t) \frac{\partial n_e(r, t)}{\partial r} + D_{e,T}(r, t) \frac{\partial T_e(r, t)}{\partial r} + \Gamma_{ECH}(r, t). \quad (1)$$

Here, $D_{e,n}(r, t)$ denotes the normal electron diffusion coefficient, while $D_{e,T}(r, t)$ does an off-diagonal element due to electron temperature gradient. Then, the diffusion equation is expressed with this electron flux $\Gamma_e(r, t)$ as

$$\frac{\partial n_e(r, t)}{\partial t} = -\frac{\partial}{\partial r} (r \Gamma_e(r, t)). \quad (2)$$

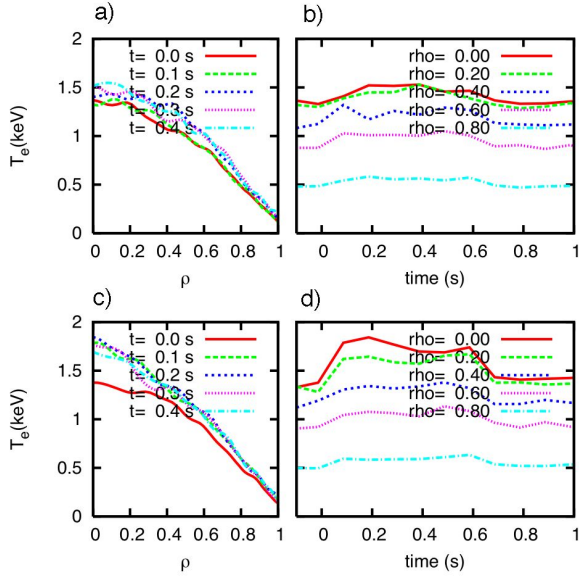


Fig. 8 Temperature profile at several time slices after ECH injection [a) and c)]. Time evolutions of the density at several spatial points b), and d) for ripple top [a) and b)] and bottom [c) and d)] heating cases.

Integrating over radius of Eq. (2) gives

$$\Gamma_e(r, t) = -\frac{1}{r} \int_0^r r' \frac{\partial n_e(r', t)}{\partial t} dr'. \quad (3)$$

Thus total electron flux can be deduced from Eq. (3) by the experimentally observed quantity $n_e(r', t)$. In Fig.9 are shown the change in the particle flux deduced from Eq. (3) for the ripple a) top and b) bottom cases. Fast increase of the flux at $\rho > 0.3$ is clear in the ripple bottom heating case than that in the top case. The density gradient profile changes are also shown in Figs.9 c) and d) for comparison. As is expected from Eq. (1), the correlations between a) and c) or b) and d) indicate the effect of normal diffusion coefficient, but there seems no clear correlation between them. Second term in Eq. (1) describes the off-diagonal

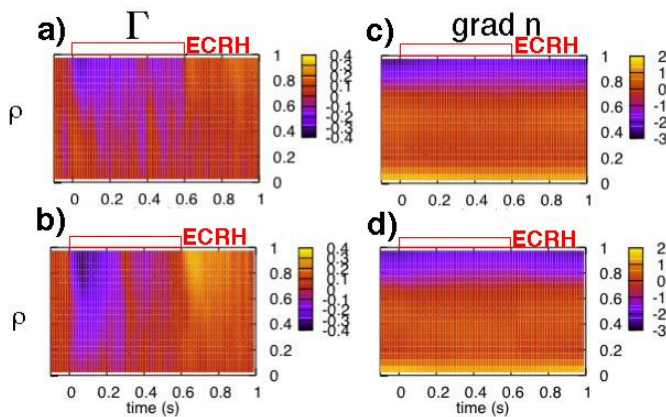


Fig. 9 Particle flux deduced from Eq. (3) for ripple a) top and b) bottom cases. c) and d) show a temporal change in the density gradient for each case.

term from the temperature gradient. As is described above, the temperature profile change occurs only at the beginning 100 ms after ECRH injection for both cases. So the correlation between the deduced flux and the temperature gradient should also be weak. These results indicate that the change in the deduced particle flux for the ripple top and bottom cases are directly driven by ECRH, although the dynamical dependence of the diffusion coefficient on the temperature and its gradient, off-diagonal term and the effect of the radial electric field should be considered more carefully.

4 Conclusion

By applying ripple top and bottom second harmonic ECRH, the density clamping phenomena are investigated. From the comparison of the density clamping between different ripple cases ($R_{ax}=3.60$ and 3.75 m), ECRH physics that is perpendicular acceleration of the electron, is shown to play an important role in the clamping phenomena. This indicates that the ECRH can be one of a nobis to control the local density. The difference in the temporal behavior of the electron density can be explained qualitatively by the direct electron flux by ECRH due to the enhanced ripple loss. The effect of the formation of radial electric field might have mitigated the degradation. Experimental and theoretical investigations of the effect of radial electric field are left for future work.

5 Acknowledgement

The authors would like to express their thanks to the continuous efforts of technical staff of ECRH and LHD to perform the experiments. This work is mainly performed under budget code NIFS05ULRR501-3.

- [1] K. Ito *et al.*, J. Phys. Soc. Japan **58**, 482 (1989).
- [2] H. Sanuki *et al.*, Phys. Fluids, **B2**, 2155 (1990).
- [3] H. Idei *et al.*, Fusion Engineering and Design **26**, 167 (1995).
- [4] C. Angioni *et al.*, Nuclear Fusion **44**, 167 (2004).